

## An ion gating, bunching, and potential re-referencing unit

C. J. Dedman, E. H. Roberts, S. T. Gibson, and B. R. Lewis

Citation: [Review of Scientific Instruments](#) **72**, 2915 (2001); doi: 10.1063/1.1379966

View online: <http://dx.doi.org/10.1063/1.1379966>

View Table of Contents: <http://scitation.aip.org/content/aip/journal/rsi/72/7?ver=pdfcov>

Published by the [AIP Publishing](#)

---

### Articles you may be interested in

[Accelerating Radioactive Ion Beams With REX-ISOLDE](#)

AIP Conf. Proc. **680**, 245 (2003); 10.1063/1.1619707

[Novel method for the production of finely spaced Bradbury–Nielson gates](#)

Rev. Sci. Instrum. **72**, 4354 (2001); 10.1063/1.1416109

[A crossed molecular beam apparatus using high-resolution ion imaging](#)

Rev. Sci. Instrum. **70**, 3265 (1999); 10.1063/1.1149902

[Experimental adaptive optimization of mass spectrometer ion optic voltages using a genetic algorithm](#)

Rev. Sci. Instrum. **70**, 2262 (1999); 10.1063/1.1149750

[Cooling, bunching and isobar separation of radioactive ion beams at IGISOL](#)

AIP Conf. Proc. **455**, 981 (1998); 10.1063/1.57303

---



You don't still use this cell phone



or this computer



Why are you still using an AFM designed in the 80's?



It is time to upgrade your AFM

Minimum \$20,000 trade-in discount for purchases before August 31st

Asylum Research is today's technology leader in AFM

[dropmyoldAFM@oxinst.com](mailto:dropmyoldAFM@oxinst.com)



**OXFORD**  
INSTRUMENTS

*The Business of Science®*

# An ion gating, bunching, and potential re-referencing unit

C. J. Dedman, E. H. Roberts,<sup>a)</sup> S. T. Gibson, and B. R. Lewis  
*Research School of Physical Sciences and Engineering, The Australian National University,  
 Canberra, ACT, 0200, Australia*

(Received 1 March 2001; accepted for publication 23 April 2001)

A novel design to achieve the gating, bunching, and potential re-referencing of an ion beam, suitable for use in a photofragment spectrometer, is presented. The device simultaneously performs all three functions in a simple, compact, and easily aligned unit. It requires only a single digital signal and one high voltage supply for operation, and provides higher flux density than previous designs. The unit uses lensing to perform beam gating, an approach which has not been reported previously. The design does not require grids, and does not introduce divergence into the ion beam. Experimental results for the combined gating, bunching, and re-referencing unit are presented, and compared with modeled performance. © 2001 American Institute of Physics. [DOI: 10.1063/1.1379966]

## I. INTRODUCTION

The formation of ion packets is required in many ion beam systems, particularly for time-of-flight (TOF) spectrometry.<sup>1</sup> The present work arises from the need to generate high-current, low-divergence ion packets within a photofragment spectrometer. Several methods exist for the production of ion packets with good number density and spatial characteristics. These can be grouped into two general approaches: methods which extract a temporally brief packet from a continuous or extended beam of ions, and methods which directly generate a temporally brief source of ions.

The generation of an ion packet from a temporally extended or continuous source has generally involved the deflection of the beam across an aperture.<sup>1-4</sup> The most common method of ion-beam gating is the differential impulse sweep method (DISM),<sup>2,4</sup> in which a pair of deflector plates sweeps the ion beam across the axis of the beam line. An aperture between the deflector plates and the detector, and the magnitude of the field with which the beam is swept, define the duration of the ion packet after the aperture.

The DISM is suited to high-resolution systems, since a very short pulse is generated easily. The expression for the temporal base width  $\Delta t$  is given by

$$\Delta t = \frac{(B+S)A}{LV_d} \sqrt{\frac{V_a M}{2e}}, \quad (1)$$

where  $B$  is the beam width,  $S$  is the aperture width,  $A$  is the separation of the deflection plates,  $L$  is the drift length,  $M$  is the mass of the species of interest,  $V_a$  is the acceleration voltage, and  $V_d$  is the deflection voltage (which switches from  $+V_d$  to  $-V_d$ ). Using the dimensions and voltages of Yefchak *et al.*<sup>4</sup> in Eq. (1) ( $L=2.1$  m,  $S=6.35$  mm,  $B=0.13$  mm,  $A=13$  mm,  $V_d=63$  V), and assuming  $O_2^-$  ions at  $V_a=8$  keV, it follows that  $\Delta t \approx 23$  ns. At the prevailing ion speed of  $135\,000$  ms<sup>-1</sup>, this corresponds to an ion-bunch

length of 3 mm, which is approximately the diameter of the typical laser beams used in laser spectroscopy. The mass resolving power (MRP)  $R$  is defined here as

$$R = \frac{M'}{M' - M}, \quad (2)$$

where  $M$  and  $M'$  are slightly different masses that are just resolved. Yefchak *et al.*<sup>4</sup> determined experimentally an MRP of  $>500$  for fragments of a heavy organic molecule, compared with a theoretical upper limit of  $>700$  for a linear TOF layout. By using a reflectron<sup>5</sup> to increase the drift length and remove energy dispersion effects, the MRP can be increased to  $>4400$ .<sup>4</sup>

The DISM switch produces a small, low-current ion packet with low duty cycle and triangular intensity-versus-time profile,<sup>4</sup> because only ions in the middle few millimeters of the deflector plates satisfy the conditions to pass through the aperture, limiting the available beam current. In addition, only those ions exactly at the center of the deflection plates when the beam is modulated do not receive any transverse velocity at all (assuming the positive and negative sweep voltages are equal in magnitude), so the gating process imparts an overall divergence to the ion packet.

Other methods of ion-beam gating are used less commonly. One such method is the use of an interleaved comb.<sup>6,7</sup> Two sets of wire grids are held at the same potential as the ion beam (gate open), or at different, opposing potentials (gate closed). When the gate is closed, the ions are deflected to either side of the beam axis. This method has been applied to the selection of a specific mass from a beam whose bunching is defined by the duration of a desorption laser pulse,<sup>7</sup> with an experimental MRP of 167 and a theoretical MRP of 300. Stoermer *et al.*<sup>6</sup> subsequently obtained a MRP of 280 using two gates in a laser desorption and ionization TOF mass spectrometer. For such an application, the small along-axis dimension of the interleaved comb compared with a conventional deflection-plate structure is an advantage in selecting a specific mass-to-charge ( $M/z$ ) ion packet, particularly as the physical separation of species decreases with increasing  $M/z$ . The use of opposing voltages on the grid

<sup>a)</sup>Electronic mail: ehr121@rsphysse.anu.edu.au

pairs results in reduction of the deflection field within a much shorter distance from the center of the grids than is possible with a deflection-plate assembly.<sup>7</sup>

Becker and Cheshnovsky<sup>8</sup> have reported the use of a combined lens and stopping grid to allow the transmission of a selected mass while blocking masses of lower energies. This works by timing the arrival of the desired (parent) ion, and applying a potential sufficient to stop lower-energy species (e.g., daughter fragments) while transmitting the parent ions. The mass gate acts as a lens for ions of interest, and a mirror for lower-energy ions. A MRP of about 20 has been demonstrated for the separation of  $\text{Xe}_{18}\text{I}^-$  and  $\text{Xe}_{19}\text{I}^-$ .<sup>8</sup>

Whaley, Goodman, and Getty<sup>9</sup> used a gating grid to extract ions for a defined time period (ranging from 50–400 nm) from a continuous plasma source into a TOF drift tube. The high magnetic field associated with the plasma source required the use of a compact grid rather than a deflection approach,<sup>2</sup> which would have greater susceptibility to magnetic fields. By varying the gating-grid voltage, it was also possible to determine the energy distribution for a given species. Whaley and co-workers<sup>9</sup> reported a MRP of about 35 for their spectrometer.

Cowen and Coe<sup>1</sup> have developed a different beam-energy modulation approach, in which a packet of ions from a continuous beam is accelerated to a slightly higher energy than the main beam, by using a variation of the potential-switch principle. Ions inside a cylinder when the potential is raised have a higher energy than the main beam. Two such cylinders are used, separated by a known distance, and with acceleration wave forms offset by a variable time delay. For a given time delay between the two electrodes, only ions of a given mass will be accelerated at both electrodes. A third electrode is held at a potential so as to stop ions at the energy of the main beam, and those which have only been accelerated at one of the two electrodes. The output is a steady state, mass-filtered current, and mass spectra can be recorded by varying the time delay between the accelerating wave forms at each electrode. Such an arrangement can be added usefully to an existing continuous beam line. The MRP of 23 reported for this method<sup>1</sup> is insufficient for many applications, and, as the packet length is shortened to increase resolution, the number of ions available will decrease.

An alternative approach to pulsed TOF mass spectrometry is the modulation of a continuous ion beam, with corresponding demodulation at the detector.<sup>10,11</sup> The beam is encoded with a pseudo-random sequence of “on” and “off” pulses, by a modulator consisting of an interleaved comb and slit. The signal is acquired synchronously with the modulation of the ion beam. The received signal is deconvolved with a fast Hadamard transform,<sup>12</sup> to extract a TOF spectrum. Duty cycles of 50% can be achieved with this approach. Brock, Rodriguez, and Zare<sup>10</sup> reported MRPs of >2000 for such an approach, and, like Stoermer *et al.*,<sup>6</sup> noted the performance limitations associated with the rise and fall times of the deflector voltages, which were typically 10 ns. In applications where the ion source and laser beams are both pulsed, such as the present application, the technique of beam encoding cannot be applied, because the duty

cycles for both the source and laser beams are typically very low.

Direct generation of temporally brief ion sources will typically use a short laser pulse,<sup>13,6</sup> a short pulse of charged particles such as electrons,<sup>14</sup> or the pulsed output from a synchrotron<sup>15</sup> to generate an ion packet. Since the ion-generation process is brief, no further temporal manipulation of the ion packet may be required, unless the selection of a specific ion species is needed.<sup>6,8</sup> Laser-based ion sources give rise to large ion-energy distributions,<sup>13,16</sup> which require the use of a reflectron configuration<sup>5,16,17</sup> or a high ion-extraction field, or both, to retain mass resolution.

Here, we describe a gating, bunching, and switching unit optimized for use in pulsed-source experiments in which the source duration is longer than the desired ion packet duration, and high instantaneous ion currents are required, rather than high mass resolution capability.

## II. DESIGN REQUIREMENTS

We are developing a fast-beam photofragment spectrometer, similar in design to that described by Continetti *et al.*<sup>18</sup> The photofragment spectrometer operates in pulsed mode, using a discharge source similar to that of Osborn.<sup>19</sup> The source uses a solenoid-operated pulsed valve to admit a brief pulse of high pressure gas, which is ionized by an electrical discharge across electrodes placed in the expanding gas jet. This provides a source of cold ions, with consequently low thermal motion, leading to a narrow energy distribution. The resultant ion pulse has a duration of about 50  $\mu\text{s}$  when measured at the gating, bunching, and potential re-referencing unit. The ion optics selects and accelerates a packet of negative ions which are brought to a focus between photodetachment and photolysis laser beams, having diameters of about 2 mm and pulse durations of about 25 ns. The photodetachment laser beam removes the electrons from the ions in the beam, leaving a neutral beam, which intersects the photolysis laser beam. Any remaining ions are electrostatically deflected from the beam axis. The resulting neutral fragments from photolysis are detected on a time- and position-sensitive detector, while the unfragmented neutrals are blocked from the detector by an on-axis beam block. The experiment is designed to operate at a repetition rate of 50 Hz. We require that the instrument provide an energy resolution  $E/\Delta E$  of better than 100:1 in photofragmentation mode. The key requirements for the ion-optic system are discussed in the following subsections.

### A. Mass selection

A TOF method of mass selection is used in our instrument, which requires the production of a short, well defined ion packet. Differing ion masses within the packet will have different velocities but identical energies (neglecting any source energy distribution), and will therefore separate in time and space along the drift section of the instrument. The ion source provides a pulse with a duration of tens of microseconds, so the ion optics is required to select, or gate, a brief subset of this extended pulse, to match the laser pulse duration.

The discharge source generates a wide range of species associated with both the gas used in the discharge, components of the discharge source (e.g., fluorine from the Teflon insulation) and contaminants in the feed gas and the vacuum system (such as vacuum pump oil), which may be separated by only one or a few atomic mass units. The typical MRP required in the TOF mass selection is on the order of 100, which is much less than that required for conventional TOF systems, where MRPs  $>1000$  are sought for the spectrometry of heavy organic species.<sup>16</sup>

### B. Potential re-referencing

To simplify the electrical design of the ion optics, it is desirable to re-reference the ion bunch to ground through the use of a potential switch,<sup>20</sup> and this method is easily exploited due to the pulsed nature of the system. By rapidly changing the potential of a cylinder from the beam potential to ground, ions within the cylinder which have entered at the beam potential leave it at ground potential, but with unchanged kinetic energy. This allows subsequent ion optics to be designed around ground potential, rather than at successively higher voltages, and allows a beam re-referenced to ground to propagate in the unshielded beam-line vacuum enclosure.

### C. Axial bunching

Low photofragment count rates are a significant practical problem in reported photofragment spectrometers.<sup>18</sup> The ion optics should have the highest possible efficiency to ensure an adequate density of particles at the points of laser-beam interaction. Ion density can be substantially increased by axially compressing a long ion packet (80 mm in this design), down to the dimensions of the laser beam (2 mm in this case), a factor of 40.

A typical spatial buncher consists of a pair of disks oriented to provide a uniform axial electric field, with a hole in the center of each disk to allow passage of the ion bunch.<sup>20</sup> While the packet of ions to be compressed is between the plates, a potential  $\Delta V$  of around 100 V is applied across the plates. Ions at the front of the bunch receive little additional energy, since they leave the field region almost at once. Those at the back of the bunch are accelerated by the full plate potential. The correct choice of accelerating voltage ensures that overlap of the front of the packet by the back occurs at the point where spatial focusing is desired; in our case in the laser-interaction region of the spectrometer. Previous photofragment designs<sup>18,20</sup> typically used a plate separation of 25 mm to compress a 15 mm ion bunch.

The energy difference  $\Delta E$  required to compress a bunch of ions of length  $l$  at energy  $E$  over a drift length  $L$  ( $\gg l$ ) is

$$\Delta E = \frac{2El}{L}. \quad (3)$$

The bunching process introduces a small energy spread  $\Delta E$  for ions within the ion packet, which degrades the recoil-energy resolution of the final spectrometer. This energy degradation puts an upper limit on the bunching voltage  $\Delta V$  of about 80 V or 1% of the final beam energy of 8 keV, in order

to achieve our desired final energy resolution of 100:1. The bunching voltage can be adjusted to trade-off ion intensity against the energy distribution of the ions, for different experimental requirements.

### D. Beam divergence

The energies of the neutral fragment pairs from photolysis are determined by the relative time of arrival of the two fragments, and their radial separation.<sup>21</sup> To maximize the energy resolution of the instrument, therefore, the divergence of the unfragmented neutral beam must be minimized, to minimize uncertainty in the measurement of radial separation. In addition, the angular width of the on-axis neutral beam block of the final three-dimensional photofragment detector is set by the dispersion of the neutral beam. This should be small, so that neutral fragments with small angular translation, e.g., relatively heavy fragments, can be detected. Thus, the ion optics system, and, in particular, the means of beam gating, should not induce beam divergence.

## III. DESIGN

Previous photofragment spectrometers<sup>18</sup> have used separate electrostatic devices to perform gating, bunching, and potential re-referencing. The device described here performs simultaneously all of these functions in a simple, compact, easily aligned unit, and should also provide higher flux density than previous designs. The design does not introduce divergence into the ion beam, and also simplifies the synchronization of timing in the photofragment spectrometer.

### A. Operating voltage

A final ion-beam energy of 8 keV is chosen to provide high quantum efficiency for the detection of the neutral fragments by the microchannel-plate detector.<sup>18,22</sup> Unlike previously reported photofragment spectrometers in which the ion beam is accelerated to its final energy of around 8 keV and then gated and bunched,<sup>18</sup> in this design the gating, bunching, and TOF drift occurs at an intermediate energy of 1 keV, with the selected bunch then accelerated to the final 8 keV energy. As with previous designs, there is a trade-off between mass resolution, energy spread induced in the buncher, and the attainable ion density at the photodetachment laser. A drift energy of only 1 keV maximizes the drift time, permitting an extremely long (80 mm) packet to be axially compressed to 2 mm without excessive energy spread. To compare the utility of the present gating, bunching and potential re-referencing unit with a conventional DISM gating unit operating at the final beam energy, we propose a figure of merit  $G$  applicable to the photofragment instrument, where flux density is more important than very high mass resolution

$$G = \frac{N}{\Delta E}, \quad (4)$$

where  $N$  is the number of ions in the bunch, and  $\Delta E$  is the energy spread due to bunching.

The number of ions in the bunch is given in terms of the bunch energy  $E$ , the length of the buncher  $b$ , and the ion flux  $dN/dt$  as

$$N = \frac{dN}{dt} b \left( \sqrt{\frac{2E}{M}} \right)^{-1}. \quad (5)$$

Combining this with Eq. (3) gives

$$G = \frac{dN}{dt} b \left( \sqrt{\frac{2E}{M}} \right)^{-1} \frac{L}{2Eb} \propto \frac{L}{E^{3/2}}. \quad (6)$$

The permissible energy spread  $\Delta E$  introduced by axial bunching is a constant dictated by the required recoil-energy resolution of the photofragment spectrometer. Compared with a system such as that used by Continetti *et al.*,<sup>18</sup> employing the DISM and a TOF drift at 8 keV energy, the potential gain in flux density in the current system with TOF mass separation performed at an intermediate energy of 1 keV is  $8^{3/2}$ , or about 25.

It is impractical to gain further improvement by operating at  $<1$  kV beam energy, due to the difficulties of transporting a low-energy beam with a correspondingly large divergence. The beam divergence follows the relationship

$$B\theta\sqrt{E} = \text{constant}, \quad (7)$$

where  $B$  is the beam diameter,  $\theta$  is the beam divergence, and  $E$  is the drift energy.<sup>23</sup>

The present system uses a number of 40-mm-diam ion lenses to focus the ion beam along the 2 m drift region. At energies  $<1$  kV, modeling (Sec. III G) indicates that these lenses could not accommodate the resultant large beam diameter or divergence, and flux is lost. In addition, at these low energies, mass separation becomes poor if the energy spread due to the ion source is significant compared with the drift energy. Consequently, the choice of 1 kV TOF energy, with subsequent acceleration to a final energy around 8 keV, is appropriate for this instrument.

## B. Mass resolution

Ion packets of different mass are resolved if, at the end of the TOF section, the separation between packets is equal to the length of the packets. In practice, the diameter of the photolysis laser beam should also be the same as the packet length to maximize overlap between laser beam and ion packet. Considering two successive ion packets of length  $S$ , containing ions of mass  $M$  and  $M'$ , the MRP, assuming minimal energy spread from the ion source, is calculated as follows.

An ion of mass  $M$  with kinetic energy  $E$  has a speed

$$v_M = \sqrt{\frac{2E}{M}}. \quad (8)$$

To resolve a second mass  $M'$ , it must travel only a distance  $L - S$ , determined by the ratio of the masses

$$\frac{(L - S)}{L} = \sqrt{\frac{M}{M'}}. \quad (9)$$

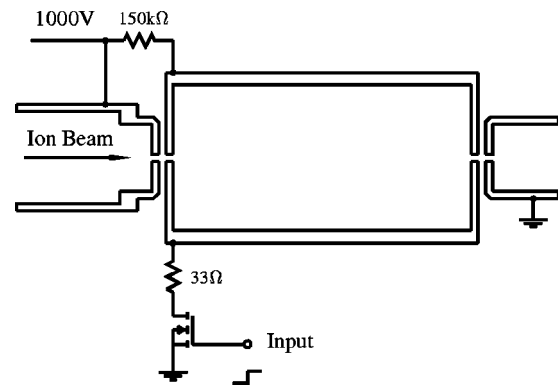


FIG. 1. Simplified schematic of the gating and potential re-referencing unit. A single FET switch and biasing network are used to switch the cylinder of the re-referencing unit between 1 kV and ground. The first and last apertures are held at 1 kV and ground, respectively. The bunching function is omitted for clarity.

Combining Eqs. (9) and (2) leads to the expression (to the first order, for  $L \gg S$ )

$$R = \frac{L}{2S}. \quad (10)$$

Thus the MRP is determined by the drift length and the extent to which the packet length can be reduced by axial bunching. For the values of  $L$  and  $S$  in the present case of 2000 and 2 mm, respectively, the resulting MRP is  $R \approx 500$ , well in excess of the typical requirement of 100 discussed in Sec. II.

## C. Potential switch design

The mechanism used here for rereferencing the beam is the same as used elsewhere.<sup>20,24</sup> The potential-switch cylinder is biased by a high-voltage supply through a current-limiting resistor, and a field-effect transistor (FET) switch is used to rapidly ground the cylinder. To facilitate axial bunching within the same unit, our ‘‘cylinder’’ is in fact constructed from a series of closely spaced aluminum rings. For the purposes of re-referencing, this structure can be regarded as an enclosed cylinder with apertures at each end, as shown in Fig. 1.

Normally, the potential-switch cylinder is substantially longer than the ion packet of interest within the cylinder (typically 250 mm for a 20 mm ion packet), and, therefore, a very modest switching speed (e.g., 230 ns) is adequate.<sup>24</sup> The switching-speed requirement for this unit, where electrically grounding the cylinder simultaneously defines and re-references the ion packet, is very stringent by comparison, and can be estimated from the dimensions of the switch and the speed of the ions of interest. For a light ion such as  $\text{OH}^-$  at 1 kV, the ion speed is around  $10^5 \text{ ms}^{-1}$ . If the switch length is set to 80 mm, and we require that switching occur within 1% of this length, the required switching time becomes about 8 ns. In fact, we achieve around 3.4 ns for the potential switch and its associated electronics (Sec. V).

Typical potential-switch apertures are at least 3 mm in diameter,<sup>18</sup> and field fringing in the vicinity of the apertures causes no problem, provided that the packet of interest is

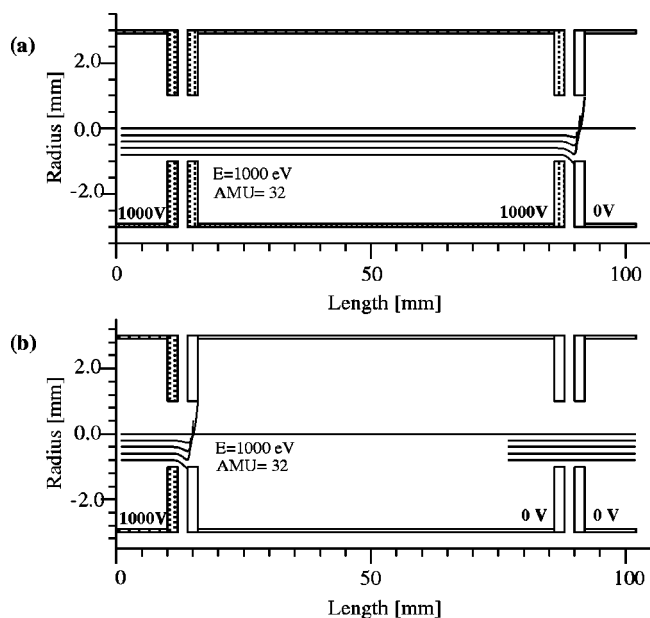


FIG. 2. (a) Model calculations of the ion beam path for the gating unit “shut” viewed as a vertical section. The central body of the unit is at 1 kV. A 1 keV 32 amu ion beam enters the unit from the left. The lens, formed by the differential voltage at the exit, deflects the ion beam, preventing the transfer of the ions into the next stage of the apparatus. Five ion paths are shown, corresponding to 0.25 mm displacements from the central axis. The unit has axial symmetry and the vertical scale has been enlarged compared to the horizontal scale, for clarity. (b) The ion beam path with the gating unit “open.” The central body of the unit is at 0 kV, and ions within the gating unit exit at ground potential and 1 keV kinetic energy. The lens, formed by the differential voltage at the entrance, deflects the ion beam, preventing the transfer of the ions into the bunching unit.

short compared with the overall cylinder length. This unit employs smaller (2 mm) apertures, to limit the field fringing which, for this composite re-referencing and gating unit, would lead to undesirable aberrations at the ends of the ion packet. This aspect is discussed further in Sec. III D. In our instrument, these relatively small apertures do not reduce the flux throughput significantly, and are beneficial for differential pumping between adjacent vacuum chambers. The apertures also serve to limit the propagation of stray ions through the rest of the beam line.

#### D. Gating unit

The gating unit reported here is designed to select a physically defined packet of all species from the ion source, thus defining the start time for the separation of masses over the TOF drift length. The packet should contain as many ions as possible, in order to maximize the subsequent number of neutrals for photofragmentation. We also require that these ions have limited lateral dispersion, and that they provide good physical overlap with the dimensions of the laser beams.

Gating is performed by a pair of small cylindrical lenses, each consisting of a pair of disks with small (2.0 mm diameter) holes, separated by 2.0 mm. The lenses, or ion gates, are located at each end of the 80-mm-long unit, as shown in Fig. 2. When the two elements of a lens are at the same potential as the beam, no lensing is performed and the ion gate is open. When one of the lens elements is at a distinctly

different potential, a strong lensing action results in the deflection of all ions from the beam axis, and the ion gate is shut. In theory, ions exactly on axis are not deflected, but, in practice, the number of such undeflected ions is immeasurably small due to the extremely strong lensing action.

Prior to generation of an ion packet, the FET switch is off, so that all parts of the unit are at 1 kV potential, except for the grounded aperture at the output end. The input lens is therefore open, so the ion beam travels undeflected into the unit, but the output lens is closed, as shown in Fig. 2(a). To generate an ion packet, the FET rapidly switches the cylinder to ground, resulting in the simultaneous closing of the input gate and opening of the output gate, as shown in Fig. 2(b). The packet of ions that was within the cylinder at the time of switching will continue through the (now open) output aperture, and along the beam line, thus defining the start of the TOF process. In addition, the ion packet has been conveniently re-referenced to ground potential. Thus, the dual functions of gating and potential re-referencing are performed with a compact, easily fabricated structure, which is readily driven by a single FET triggered by a delay circuit within the spectrometer.

The use of cylindrical lenses to perform gating for TOF spectrometers has not been reported previously. As noted above, the use of a mass gate-energy discriminator,<sup>8</sup> and interleaved comb deflection<sup>7</sup> rely on lensing to deflect or stop the beam, but both require grids or meshes, and are more complex than the approach used here.

End effects in the lenses impart an energy spread to a very small portion of the bunch. This effect is minimized by using small lens apertures which reduce the axial distance over which lensing takes place, and by using a fast switching circuit. Both modeling (Sec. III G) and measurement (Sec. V) confirm this characteristic. The uncompressed packet length is set by the length of the bunching assembly, rather than the deflection field, used in the DISM.<sup>2</sup> As with the DISM, separation of the ion bunch into different masses is achieved by the TOF along a drift tube, but no defining aperture is needed because the ions are either on-axis, or deflected totally out of the beam line by the extremely strong lensing action of the ion gates.

The gating unit reported here is better suited to photofragment spectroscopy than one based on the DISM, which operates by introducing a transverse velocity component to the beam. In a typical TOF mass spectrometer using the DISM, the detector would be placed immediately after the final packet-defining aperture. In a photofragment spectrometer, however, the beam continues to diverge for several meters after the final aperture. The system described here imparts no transverse velocity component to the packet, and thus does not suffer from this form of beam aberration, and the consequent impact on measurement noted in Sec. II D.

#### E. Buncher

For our requirement of a long (80 mm) uncompressed ion packet length, a conventional parallel plate buncher would be physically large and awkward to implement. Instead, only a slight modification of the combined gating and

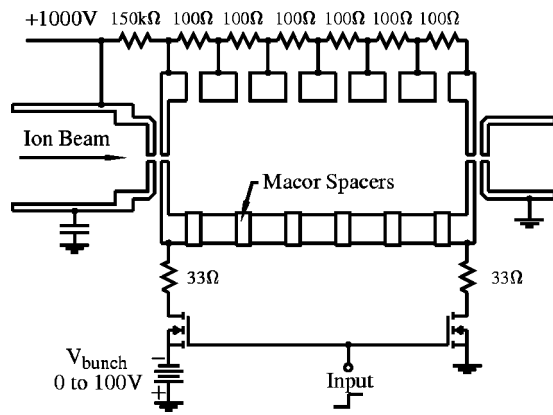


FIG. 3. Sectional view of the combined gating, bunching, and potential re-referencing unit. The chain of resistors which set up the bunching field, and the pair of FET switches, are shown. The degree of bunching is varied with the variable bunching voltage,  $V_{\text{bunch}}$ . FET switching circuit details, such as gate drive pulse transformers, have been omitted for clarity.

re-referencing unit of Fig. 1 is required to add the capability for axial bunching. Instead of a continuous cylinder, we use a series of aluminum rings, closely spaced to prevent field penetration into the active region of the buncher, as shown in Fig. 3. This structure also provides reasonable conductance for vacuum pumping. The rings are biased through a series chain of resistors attached directly to the rings to minimize external electrical connections through the vacuum envelope, and minimize system capacitance. Modeling shows that this compact structure provides an extremely uniform axial electric field when a fixed voltage is applied across the resistor chain. Reflectron designs typically also use a series of biased rings to establish a uniform field.<sup>5,17</sup> Two FET switches are used, with the first FET switching to  $-V_{\text{bunch}}$  rather than to ground.

In operation, the FETs are switched simultaneously, with the output aperture switched to ground and the input aperture switched to  $V_{\text{bunch}}$ , adjustable from 0 to  $-100$  V. In this manner, axial bunching is performed, in addition to the gating and potential re-referencing described in Sec. III D, for the cost of only one additional FET switch. In our implementation, the uncompressed packet length is set by the physical length of the unit, which can be removed easily from the spectrometer and replaced by one of different length. It is also possible to shorten the packet length by delaying the opening of the output gate with respect to the closing of the input gate, although it should be noted that the physical length of the shortened packet would then be a function of ion mass.

#### F. Fast high voltage switch

The successful operation of the combined gating, bunching, and re-referencing unit relies on the ability to switch from 1 kV to ground within a few nanoseconds. FETs are used as the main 1 kV switches, with their gates driven by stepdown bifilar-wound toroidal pulse transformers with multiple parallel windings. These are driven by a single FET operating at 80 V, which is driven by a FET driver chip. The circuit layout, bypassing, and construction of the pulse transformers are critical to obtaining the measured switching time

of 2.5 ns for the circuit without the switching electrodes attached. The design and construction of this switch are detailed elsewhere.<sup>25</sup>

#### G. Computer modeling

The performance of the photofragment spectrometer has been modeled through locally developed software which allows the physical dimensions of the elements of the ion optics chain, and their voltages at a given time, to be defined. The energies and masses of ions can be defined, and the paths of these ions through the experiment are modeled. The software determines the electric fields at all points on a mesh within the experiment, and determines the forces on the ions as they move through the beam line. The same software has been used to determine the type and location of the Einzel lenses in the transport optics of the instrument, as well as the gating, bunching, and potential switching designs. Second-order effects in the design, such as the behavior of ions adjacent to the ion-gate lenses during the switching phase, have been examined with the software, which showed that such ions are mainly deflected out of the beam and do not degrade the resolution of the instrument.

Our simulation of the behavior of a bunch of ions after a DISM gate and subsequent apertures has demonstrated the impact of the divergence introduced to the ion packet, with the consequent loss of packet intensity. It has also demonstrated the resultant triangular ion intensity profile (the convolution of the defining aperture and the ion beam profile, which were both assumed to have a diameter of 2 mm), compared with the rectangular profile from the gating unit described here.

#### IV. CONSTRUCTION

The dimensions and tolerances used in construction of the unit are relaxed, the mechanical construction is simple and compact, and the design uses common materials. The unit is made from machined aluminum disks, separated by Macor spacers, and supported on three threaded steel rods with glass tube insulation. The unit is attached, with an insulating spacer, to a disk which bolts into tapped holes in a 6 in. Conflat©Tee, to provide mechanical support and centralization in the beam line. A photograph of the finished unit is shown in Fig. 4.

The input of the unit overlaps with the output of the previous lens element, to prevent field penetration from the surrounding grounded vacuum structure. At the output, the ion bunches are at ground potential, and can propagate through the drift region of the spectrometer without further shielding.

Resistors are soldered to tags on each disk to provide the axial bunching field. The grounded output-aperture lens disk is directly connected to the heavy grounded mounting flange that physically supports the unit. The input-aperture disk is capacitively bypassed to ground through three heavy rods around the outside of the unit. The diameter of the mating faces of the input- and output-aperture lens disks are stepped

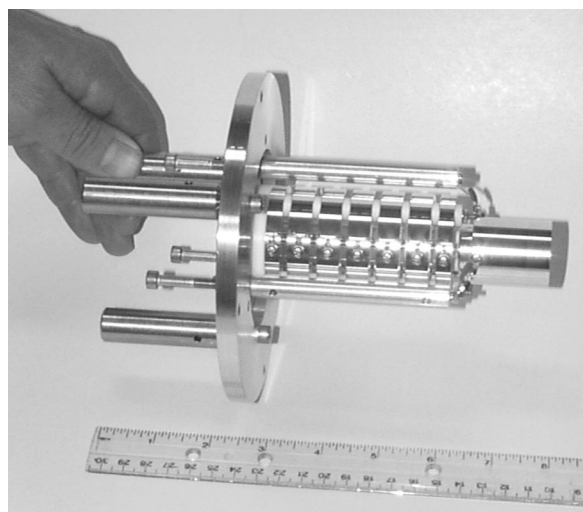


FIG. 4. Final gating, bunching, and potential rereferencing unit, demonstrating the compact construction.

down from 25 to 12.5 mm to reduce capacitance between the switch elements while still preventing field penetration into the switching region.

The FET switching unit provides an adjustable input delay of 0–100  $\mu\text{s}$ , so that the opening of the unit can be delayed with respect to the firing of the ion source, as well as an adjustable bunching voltage of 0–100 V. The FET switches remain on for a fixed delay of 3  $\mu\text{s}$ .

In principle, it should be possible to build an equivalent gating, bunching, and potential switching system using DISM deflection plates with separate buncher, and separate potential switch, with similar performance. In practice, the DISM deflection plates, separate buncher, and separate potential switch would each need to be several hundred millimeters long to accommodate ion packets up to 100 mm long, making physical implementation difficult. In comparison, our single combined unit is only 100 mm in length.

## V. PERFORMANCE

The switching speed, efficiency of aperture-lens-based switching, and the duration of unbunched and bunched ion packets were measured. By careful design of the switching electronics, and minimizing the lengths of connections from the switching FETs to the active elements, very fast switching speeds with low ringing have been achieved. A typical switching wave form is shown in Fig. 5, demonstrating a rise time of 3.4 ns, and ringing of <10% for the switching electronics when coupled to the gating, bunching, and potential re-referencing unit. Such fast switching is possible because only a single FET stage is required, rather than multiple FETs with coupling transformers that have been required for higher-energy ion beams.<sup>18</sup>

The transfer function of the lens switches was assessed by measuring the beam current at the output of the switching unit as a function of the voltage difference across the lens elements. The output beam current was measured with a Faraday cup, and the resulting switching function is shown in Fig. 6. Two characteristics are noted. First, the switch cuts off entirely for voltages below 10% of the fully open voltage,

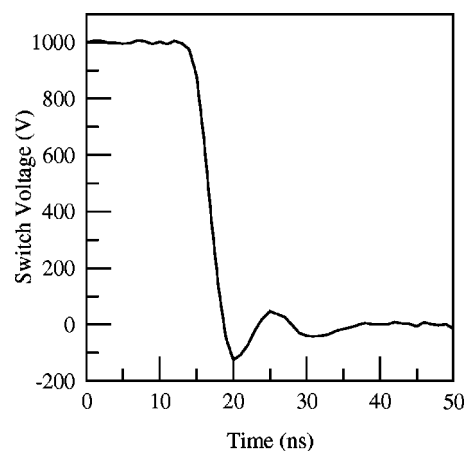


FIG. 5. Switching wave form, measured at the bunching unit, showing fast rise time.

and second, the switch is largely shut even at 20% of the operating voltage, when only 1.5% of the nominal flux is transmitted. This latter characteristic means that, even if the switching electronics leads to ringing at the 10%–20% level, this will not lead to ragged ends for the ion bunches, since the switch will remain effectively shut.

The bunching characteristics of the unit were assessed by comparing the amplitude and duration of selected ion packets, measured with a high gain microchannel-plate detector, with its anode directly coupled to the input of an oscilloscope, at the end of a 1.654 m drift tube. The results are shown in Figs. 7(a) and 7(b), in which a  $^{16}\text{O}^-$  ion pulse is shown in uncompressed and compressed form, respectively. The rectangular shape of the ion pulse from the gating unit can be clearly seen in the uncompressed pulse. The duration of the compressed pulse is only 1/40 of that of the uncompressed pulse, while its amplitude is 40 $\times$  that of the uncompressed pulse, in agreement with prediction.

The resolution of the system can be estimated by examining the separation of adjacent masses, shown in Fig. 8. The masses from 16 to 19 amu are well resolved. The separation between  $^{18}\text{O}^-$  and  $^{19}\text{F}^-$  is about 10 $\times$  the width of the peaks, indicating a MRP>280. (The intensity of the  $^{16}\text{O}^-$  signal is

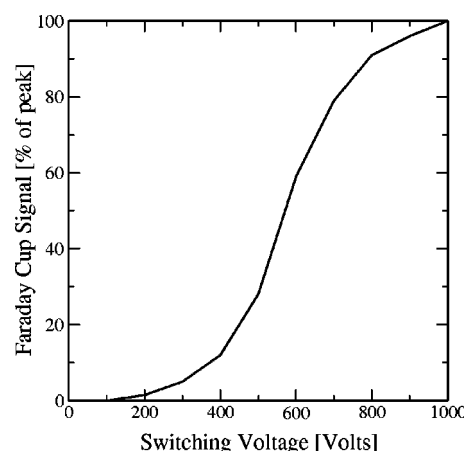


FIG. 6. Switching function for aperture lens switch. The cutoff is virtually complete, even at 20% full voltage, minimizing the importance of ringing in the switching wave form.

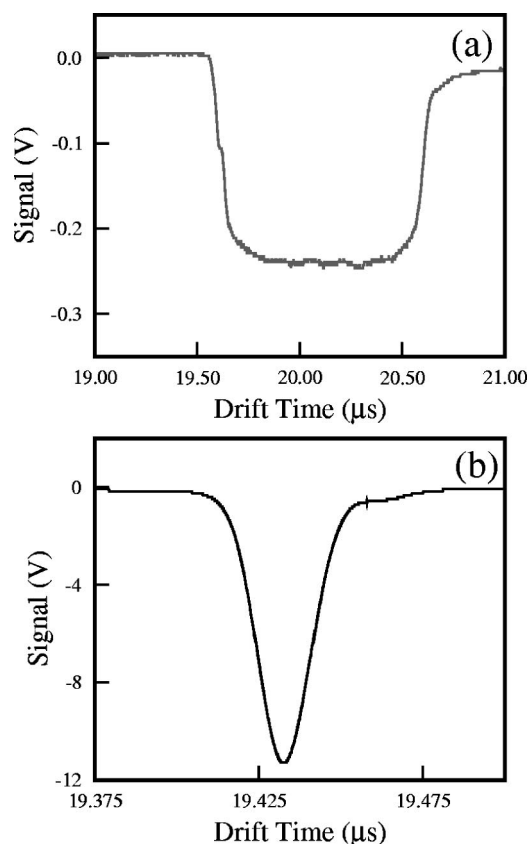


FIG. 7. (a) Signal from the  $O^-$  ion, measured with a microchannel-plate detector at 1654 mm from the gating, bunching, and re-referencing unit. (b) The same  $O^-$  pulse as in (a), with the bunching voltage applied. Note the decrease in duration and corresponding increase in amplitude of the signal.

much greater than that of the other ions in Fig. 8, so its apparent signal width is disproportionately greater.) The difference between the predicted MRP of 500 and the resolution measured here is due to the shorter drift length, the finite energy spread in the ion source, and bandwidth limitations in the 100 MHz oscilloscope used for the measurement. The  $^{16}O^-$  and  $^{18}O^-$  ion signals were measured, from the oscilloscope screen as 7.0 V and 16 mV, respectively, with a ratio of approximately 440:1, which is in reasonable agreement

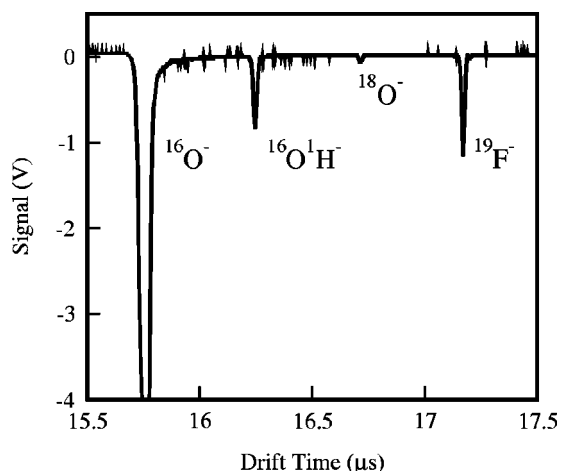


FIG. 8. A mass spectrum with bunching applied. Masses 16–19 are resolved. (The  $O^-$  signal is clipped to  $\approx 10\%$  of its actual value).

with the natural isotopic ratio of 489.2.<sup>26</sup> The ion source was optimized independently for each ion species, which is a probable cause for the difference between the measurement and the accepted value.

The number of ions in the pulse shown in Fig. 7(a) can be estimated from the duration (1  $\mu s$ ) and amplitude (0.24 V) of the pulse, the terminating resistance at the oscilloscope (50  $\Omega$ ), and the gain and quantum efficiency of the microchannel plate. The latter two are estimated, based on the manufacturer's typical values,<sup>22</sup> at  $10^6$  and 50%, respectively. The pulse shown has approximately 55 000 ions. It should be stressed that this is a preliminary value, with no optimization of the fore optics, or the skimmer of the photo-fragment instrument, undertaken.

## ACKNOWLEDGMENTS

The authors acknowledge the assistance of Professor S. J. Buckman in the development of the design of the ion optics. This work is funded by a Major Equipment Grant from the Australian National University. One of the authors (E.H.R.) is the recipient of an Australian Postgraduate Award.

<sup>1</sup>K. A. Cowen and J. V. Coe, *Rev. Sci. Instrum.* **61**, 2601 (1990).

<sup>2</sup>J. M. B. Bakker, *J. Phys. E* **6**, 785 (1973).

<sup>3</sup>J. M. B. Bakker, *J. Phys. E* **7**, 364 (1973).

<sup>4</sup>G. E. Yefchak, G. A. Schultz, J. Allison, C. G. Enke, and J. F. Holland, *J. Am. Soc. Mass Spectrom.* **1**, 440 (1990).

<sup>5</sup>B. A. Mamyrin, V. I. Karataev, D. V. Shmikk, and V. A. Zagulin, *Sov. Phys. JETP* **37**, 45 (1973).

<sup>6</sup>C. W. Stoermer, S. Gilb, J. Friedrich, D. Schooss, and M. M. Kappes, *Rev. Sci. Instrum.* **69**, 1661 (1998).

<sup>7</sup>P. R. Vlasak, D. J. Beussman, M. R. Davenport, and C. G. Enke, *Rev. Sci. Instrum.* **67**, 68 (1996).

<sup>8</sup>I. Becker and O. Cheshnovsky, *Rev. Sci. Instrum.* **68**, 4625 (1997).

<sup>9</sup>D. R. Whaley, T. P. Goodman, and W. D. Getty, *Rev. Sci. Instrum.* **60**, 358 (1989).

<sup>10</sup>A. Brock, N. Rodriguez, and R. N. Zare, *Rev. Sci. Instrum.* **71**, 1306 (2000).

<sup>11</sup>A. Brock, N. Rodriguez, and R. N. Zare, *Anal. Chem.* **70**, 3735 (1998).

<sup>12</sup>N. J. A. Sloane, in *Fourier, Hadamard and Hilbert Transforms in Chemistry*, edited by A. G. Marshall (Plenum, New York, 1982).

<sup>13</sup>W. B. Brinckerhoff, G. G. Managadze, R. W. McEntire, A. F. Cheng, and W. J. Green, *Rev. Sci. Instrum.* **71**, 536 (2000).

<sup>14</sup>C. Ma, C. R. Sporleder, and R. A. Bonham, *Rev. Sci. Instrum.* **62**, 909 (1991).

<sup>15</sup>O. Hemmers, S. B. Whitfield, P. Glans, H. Wang, D. W. Lindle, R. Wehlitz, and I. A. Sellin, *Rev. Sci. Instrum.* **69**, 3809 (1998).

<sup>16</sup>R. Cotter, *Time-of-Flight Mass Spectrometry: Instrumentation and Applications in Biological Research* (American Chemical Society, Washington, 1997).

<sup>17</sup>T. Bergmann, H. Goehlich, T. P. Martin, and H. Schaber, *Rev. Sci. Instrum.* **61**, 2592 (1990).

<sup>18</sup>R. E. Continetti, D. R. Cyr, D. Osborn, D. Leahy, and D. M. Neumark, *J. Chem. Phys.* **99**, 2616 (1993).

<sup>19</sup>D. Osborn, D. Leahy, D. R. Cyr, and D. M. Neumark, *J. Chem. Phys.* **104**, 5026 (1996).

<sup>20</sup>L. A. Posey, M. J. DeLuca, and M. A. Johnson, *Chem. Phys. Lett.* **131**, 170 (1986).

<sup>21</sup>Z. Amitay and D. Zajfman, *Rev. Sci. Instrum.* **68**, 1387 (1997).

<sup>22</sup>Burle Technologies, Inc. Scientific Detector Products Technical Briefs.

<sup>23</sup>D. W. O. Heddle, *Electrostatic Lens Systems* (Hilger, Bristol, 1991).

<sup>24</sup>R. E. Continetti, D. R. Cyr, and D. M. Neumark, *Rev. Sci. Instrum.* **63**, 1840 (1992).

<sup>25</sup>C. J. Dedman, E. H. Roberts, S. T. Gibson, and B. R. Lewis (unpublished).

<sup>26</sup>R. J. Donnelly, in *A Physicist's Desk Reference*, edited by H. L. Anderson (AIP, New York, 1989).